UNIVERSIDADE DE SÃO PAULO
Instituto de Ciências Matemáticas e de Computação
ISSN 0103-2577

GLOBAL DYNAMICS OF THE MAY-LEONARD SYSTEM WITH A DARBOUX INVARIANT

REGILENE OLIVEIRA
CLAUDIA VALLS

Nº 445

NOTAS DO ICMC

SÉRIE MATEMÁTICA

São Carlos – SP
Jan./2019

GLOBAL DYNAMICS OF THE MAY-LEONARD SYSTEM WITH A DARBOUX INVARIANT

REGILENE OLIVEIRA[1] AND CLÁUDIA VALLS[2]

ABSTRACT. We study the global dynamics of the classic May-Leonard model in $\mathbb{R}^3$. Such model depends on two real parameters and its global dynamics is known when the system is completely integrable. Using the Poincaré compactification on $\mathbb{R}^3$ we get the global dynamics of the classical May–Leonard differential system in $\mathbb{R}^3$ when $\beta = -1 - \alpha$, a non-integrable case. In this case it admits a Darboux invariant. We provide the global phase portrait in each octant and in the Poincaré ball, that is, the compactification of $\mathbb{R}^3$ in the sphere $\mathbb{S}^2$ at infinity. We also describe the ω-limit and α-limit of each of the orbits. For some values of the parameter α we find a separatrix cycle F formed by orbits connecting the finite singular points on the boundary of the first octant and every orbit on this octant has F as the ω-limit. The same holds for the sixth and eighth octants.

1. Introduction and statement of the main results

The Lotka-Volterra systems in $\mathbb{R}^3$

$$\dot{x_i} = x_i \left(\sum_{j=1}^{3} a_{ij} x_j + b_i \right) \qquad (i = 1, \ldots, 3).$$

were introduce by Lotka and Volterra in the twenties to describe the interaction among species, see [11, 15] and also [7]. Since their appearance they have been intensively investigated due to the fact that they are also important for describing different phenomena in biology, ecology and chemistry (see for instance [3, 5, 6, 8, 10, 12] and the references therein).

Due to its simplicity, special attention has attracted the so-called classical May-Leonard system introduced by May and Leonard in [13] which again describes a competition between three species but is a simple model with a rich dynamical behavior. This system can be written as

$$\begin{aligned} \dot{x} &= x(1 - x - \alpha y - \beta z), \\ \dot{y} &= y(1 - \beta x - y - \alpha z), \\ \dot{z} &= z(1 - \alpha x - \beta y - z), \end{aligned} \tag{1}$$

where α and β are real parameters.

2010 *Mathematics Subject Classification.* Primary 37C15, 37C10.
Key words and phrases. Lotka–Volterra systems, May–Leonard systems, Darboux invariant, phase portraits, limit sets, Poincaré compactification.

It was showed in [13] that, whenever $\alpha+\beta\neq -1$, system (1) has four singular points in $\mathbb{R}^3_+=\{(x,y,z)\in\mathbb{R}^3, x,y,z\geq 0\}$. Three of them are on the boundary of $\mathbb{R}^3_+$,

$$E_1=(1,0,0),\ E_2=(0,1,0),\ E_3=(0,0,1),$$

and the fourth one is the interior point

$$C=((1+\alpha+\beta)^{-1},(1+\alpha+\beta)^{-1},(1+\alpha+\beta)^{-1}).$$

If in addition, $\alpha+\beta>2$ and either $\alpha<1$, or $\beta>1$, then there is a separatrix cycle F formed by orbits connecting E_1, E_2 and E_3 on the boundary of $\mathbb{R}^3_+$, and every orbit in $\mathbb{R}^3_+$, except of the equilibrium point C has F as the ω-limit. Further, it was shown in [2] that in the degenerate case $\alpha+\beta=2$, the cycle F becomes a triangle on the invariant plane $x+y+z=1$ and all orbits inside the triangle are closed and every orbit in the interior of $\mathbb{R}^3_+$ has one of these closed orbits as its ω-limit. Moreover, in [2] it was studied completely the dynamics of the May-Leonard system whenever $\alpha+\beta=2$, or $\alpha=\beta$. Other dynamical aspects or other values of the parameters α,β were also considered in [1, 14] (see also the references therein).

In this paper we shall restrict to the cases where either $\alpha+\beta\neq 2$, or $\alpha\neq\beta$ and study the May-Leonard systems (1) that admit a Darboux invariant of the form $e^{st}f(x,y,z)$, where $f(x,y,z)$ is given by the product of invariant planes (see more details below). The existence of such a Darboux invariant provides information about the ω- and α-limit of all orbits of the system. We will see that the case in which there exists such an invariant in the May-Leonard model is whenever $\alpha+\beta+1=0$. We consider this case and we describe the global dynamics in the compactification of $\mathbb{R}^3$ in function of α. In particular, we will be able to provide all the ω- and α-limits of all orbits of the system in the positive octant, and so determining the initial and final evolution of the three species considered in the May-Leonard model. We recall that the global description of the flow of a differential system in $\mathbb{R}^3$ is generally very difficult. In that paper, using the Poincaré compactification and the fact that we have an invariant we are able to do it. The case $\alpha+\beta=-1$ is usually forgotten in the literature due to the fact that in that case the point C is missing and the dynamics become more complex. As far as the authors know this is the first paper in which the May Leonard problem under the above assumptions is completely studied from the dynamical point of view. We recall that loosely speaking the Poincaré ball is obtained identifying $\mathbb{R}^3$ with the interior of the 3-dimensional ball of radius one centered at the origin, and extending analytically the flow of system (1) to the boundary of $\mathbb{S}^2$ on that ball (see the Appendix for details).

2. Statements and main results

An *invariant* of system (1) on an open subset U of $\mathbb{R}^3$ is a nonconstant C^1 function I in the variables x,y,z and t such that $I(x(t),y(t),z(t),t)$ is constant on all solution curves $(x(t),y(t),z(t))$ of system (1) contained in U, i.e.

$$x(1-x-\alpha y-\beta z)\frac{\partial I}{\partial x}+y(1-\beta x-y-\alpha z)\frac{\partial I}{\partial y}+z(1-\alpha x-\beta y-z)\frac{\partial I}{\partial z}+\frac{\partial I}{\partial t}=0, \tag{2}$$

for all $(x,y,z)\in U$.

On the other hand given $f \in \mathbb{C}[x,y,z]$ we say that the surface $f(x,y,z)=0$ is an *invariant algebraic surface* of system (1) if there exists $K \in \mathbb{C}[x,y,z]$ such that

$$x(1-x-\alpha y-\beta z)\frac{\partial f}{\partial x}+y(1-\beta x-y-\alpha z)\frac{\partial f}{\partial y}+z(1-\alpha x-\beta y-z)\frac{\partial f}{\partial z}=Kf. \tag{3}$$

The polynomial K is called the *cofactor* of the invariant algebraic surface $f=0$. For more details see Chapter 8 of [4].

An invariant I is called a *Darboux invariant* if it can be written in the form

$$I(x,y,z,t)=f_1^{\lambda_1}\cdots f_p^{\lambda_p}e^{s\,t},$$

where, for $i=1,\dots p$, $f_i=0$ are invariant algebraic surfaces of system (1), $\lambda_i \in \mathbb{C}$, and $s \in \mathbb{R}\setminus\{0\}$.

Theorem 1. *The following holds for system* (1) *with either* $\alpha+\beta \neq 2$ *or* $\alpha \neq \beta$

(a) *It has a Darboux invariant of the form* $I(x,y,z,t)=e^{st}f(x,y,z)$*, where* $f(x,y,z)$ *is given by the product of invariant planes if and only if* $\alpha+\beta+1=0$.
(b) *It is invariant under the symmetry* $(x,y,z)\to(y,z,x)$.
(c) *The* ω*-limit of any of its orbits in* $\mathbb{R}^3$ *is contained in* Ω *union with its boundary at infinity in the Poincaré compactification in* $\mathbb{R}^3$*, where*

$$\Omega=\{(x,y,z)\in\mathbb{R}^3 : x=0\}\cup\{(x,y,z)\in\mathbb{R}^3 : y=0\}\cup\{(x,y,z)\in\mathbb{R}^3 : z=0\}.$$

From now on, we consider system (1) restricted to $\beta=-1-\alpha$ with $\alpha\in\mathbb{R}$, that is

$$\begin{aligned}\dot{x}&=x(1-x-\alpha y+(1+\alpha)z),\\ \dot{y}&=y(1+(1+\alpha)x-y-\alpha z),\\ \dot{z}&=z(1-\alpha x+(1+\alpha)y-z).\end{aligned} \tag{4}$$

In order to describe de global dynamics of system (4) we define the *ith*-octants, O_i, for $i=\{1,2,..,8\}$, as

$$\begin{aligned}O_1&=\{(x,y,z)\in\mathbb{R}^3 : x\geq 0,y\geq 0,z\geq 0\},\quad O_2=\{(x,y,z)\in\mathbb{R}^3 : x\leq 0,y\geq 0,z\geq 0\},\\ O_3&=\{(x,y,z)\in\mathbb{R}^3 : x\leq 0,y\leq 0,z\geq 0\},\quad O_4=\{(x,y,z)\in\mathbb{R}^3 : x\geq 0,y\leq 0,z\geq 0\},\\ O_5&=\{(x,y,z)\in\mathbb{R}^3 : x\geq 0,y\geq 0,z\leq 0\},\quad O_6=\{(x,y,z)\in\mathbb{R}^3 : x\leq 0,y\geq 0,z\leq 0\},\\ O_7&=\{(x,y,z)\in\mathbb{R}^3 : x\leq 0,y\leq 0,z\leq 0\},\quad O_8=\{(x,y,z)\in\mathbb{R}^3 : x\geq 0,y\leq 0,z\leq 0\}.\end{aligned}$$

The global dynamics of system (4) in O_1 (the positive octant) is given in the following theorem. In that theorem, we denote by O_1^+ the interior of O_1, i.e.,

$$O_1^+=\{(x,y,z) : x>0,y>0,z>0\}.$$

Theorem 2. *The following statements hold for system* (4) *restricted to* O_1 *for* $\alpha\in(-\infty,1)$*:*

(a) *The phase portraits in the Poincaré disc of system* (4) *restricted to the invariant planes are topologically equivalent to one of the phase portraits of Figure 1.*
(b) *The phase portraits of system* (4) *at the infinity of* O_1 *are topologically equivalent to one of the phase portraits given in Figure 2. More precisely,*

(b.1) *for $\alpha \leq -2$ the boundary of the infinity of O_1 is a heteroclinic cycle formed by three equilibrium points coming from the ones located at the end of the three positive half-axes of coordinates, and three orbits connecting these equilibria, each one coming from the orbit at the end of every plane of coordinates. In the interior of the infinity of O_1 there is an attractor whose orbits fill completely this interior.*

(b.2) *For $\alpha \in (-2, 1)$ the boundary of the infinity of O_1 is a graph formed by six equilibrium points all of them located at the positive half-axes of coordinates. Three of them are at the end of the axes and the other three are between them. Moreover, there are six orbits connecting these equilibria. Each of them coming from the orbit at the end of every plane of coordinates. In the interior of the infinity of O_1 there is an attractor of all the orbits coming from the equilibria at the end of every plane of coordinates.*

(c) *The phase portrait of system (4) on O_1 is giving in Figure 3 (i) when $\alpha \leq 2$ and Figure 3 (ii) when $\alpha \in (-2, 1)$. Namely,*

(c.1) *for $\alpha \leq -2$, there exists a separatrix cycle F formed by orbits connecting the finite singular points on the boundary of O_1 and every orbit on O_1, except the origin, has F as its ω-limit. The $\alpha-$limit set of the orbits on $O_1^+ \setminus F$ is formed by four equilibrium points, the origin and the three equilibria located at the end of the positive half-axes of coordinates.*

(c.2) *for $\alpha \in (-2, 1)$, there exists a graph G formed by orbits connecting the finite singular points on the boundary of O_1, except the origin. The $\omega-$limit set of every orbit on O_1, except the origin, is one of the vertices of G. The $\alpha-$limit set of the orbits on $O_1^+ \setminus G$ is formed by seven equilibrium points, the origin and the equilibria located at the end of the invariant planes.*

Since Theorem 2 provides the ω-limit and the α-limit of all orbits inside O_1 (which is the octant where system (4) has biological meaning), in that theorem we are determining all the initial and final evolution of the three species considered by system (4) according to the values of the parameter α. We recall that the statements in Theorem 2 also hold for $\alpha \geq 1$. Indeed, the dynamics for $\alpha > 1$ is the same as the one for $\alpha < -2$ reversing the time and the dynamics for $\alpha = 1$ is the same of the one for $\alpha = -2$ also reversing the time. It follows from Theorem 1 (b) that the dynamics in O_6 and O_8 are the same as the one in O_1.

Theorem 3. *The phase portrait of system (4) on O_2 is given in Figure 4 (i) when $\alpha < -2$, or $\alpha > 1$; in Figure 4 (ii) when $\alpha = -2$, or $\alpha = 1$; and in Figure 4 (iii) when $\alpha \in (-2, 1)$. More precisely, all orbits in O_2 are heteroclinic and*

(a) *for $\alpha < -2$, all orbits starting on $O_2 \setminus A$, where $A = \{z = 0\} \cup \{x = y = 0\}$, go in forward time to infinity to an equilibrium point P_0 located outside the end of the invariant planes (see Figure 4 (i)). The same holds for $\alpha > 1$ in $O_2 \setminus B$, where $B = \{x = 0\} \cup \{y = z = 0\}$.*

(b) *for $\alpha \in [-2, 1]$, all orbits starting on $O_2 \setminus \{y = 0\}$ go in forward time to infinity to the endpoint P_0 of the negative half-axes of coordinates (y-axes). See Figures 4 (ii) and (iii).*

Theorem 4. *The phase portrait of system (4) on O_3 is given in Figure 5 (i) when $\alpha < -2$, or $\alpha > 1$; in Figure 5 (ii) when $\alpha = -2$, or $\alpha = 1$; and in Figure 5 (iii) when $\alpha \in (-2, 1)$. Namely, all orbits in O_3 are heteroclinic and*

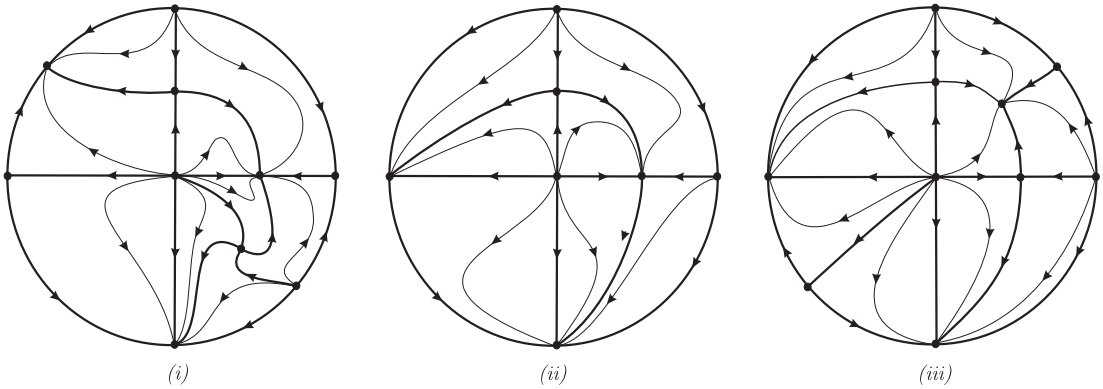

FIGURE 1. Phase portrait of system (4) on the Poincaré disc restricted to the invariant planes $x = 0$, $y = 0$ or $z = 0$ when: *(i)* $\alpha < -2$, or $\alpha > 1$; *(ii)* $\alpha = -2$, or $\alpha = 1$; *(iii)* $-2 < \alpha < 1$.

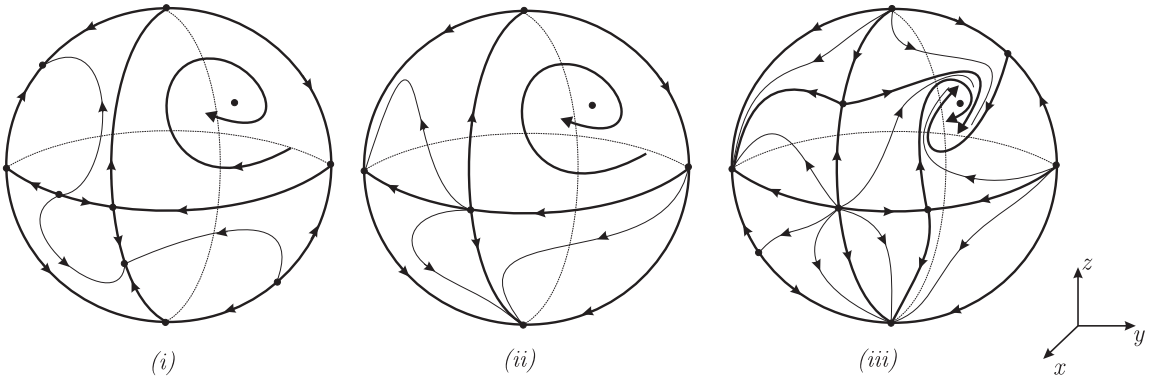

FIGURE 2. Phase portrait of system (4) on the Poincaré sphere when: *(i)* $\alpha < -2$, or $\alpha > 1$; *(ii)* $\alpha = -2$, or $\alpha = 1$; *(iii)* $-2 < \alpha < 1$.

(a) *for* $\alpha < -2$, *all orbits starting on* $O_3 \setminus \{y = 0\}$ *go in forward time to infinity to an equilibrium point* Q_0 *located outside the end of the invariant planes (see Figure 5 (i)). The same is true for* $\alpha > 1$ *in* $O_3 \setminus \{x = 0\}$.
(b) *for* $\alpha = -2$, *all orbits starting on* $O_3 \setminus \{y = 0\}$ *go in forward time to infinity to the endpoint* Q_0 *of the negative half-axes of coordinates (x-axes). For* $\alpha = 1$, *all orbits starting on* $O_3 \setminus \{x = 0\}$ *go in forward time to infinity to the endpoint* Q_0 *of the negative half-axes of coordinates (y-axes). See Figure 5 (ii).*
(c) *for* $\alpha \in (-2, 1)$, *all orbits starting on* $O_3 \setminus \{x = 0\}$ *go in forward time to infinity to an equilibrium point* Q_0 *located outside the end of the invariant planes (see Figure 5 (iii)).*

Theorem 5. *The phase portrait of system* (4) *on* O_5 *is given in Figure 6 (i) when* $\alpha < -2$, *or* $\alpha > 1$; *in Figure 6 (ii) when* $\alpha = -2$, *or* $\alpha = 1$; *and in Figure 6 (iii) when* $\alpha \in (-2, 1)$. *Namely, all orbits in* O_5 *are heteroclinic and*

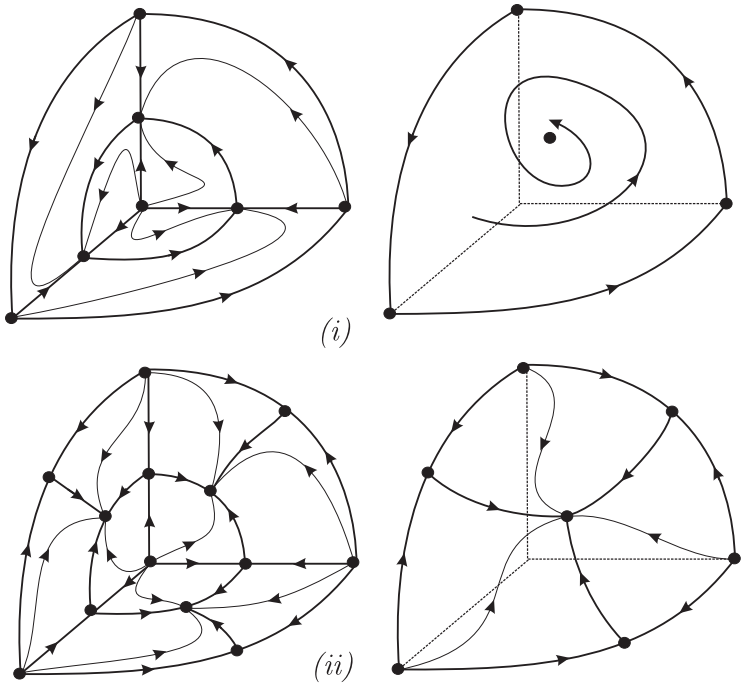

FIGURE 3. Phase portrait of system (4) in the first octant O_1: (i) for $\alpha \leq -2$ or $\alpha \geq 1$ and (ii) for $-2 < \alpha < 1$. On the left-hand side we draw the phase portrait of system (4) restricted to the positive invariant planes and on the right-hand side we draw the phase portrait of system (4) on the Poincaré sphere in O_1.

(a) *for $\alpha < -2$, all orbits starting on $O_5 \backslash C$, where $C = \{x = 0\} \cup \{y = z = 0\}$, go in forward time to infinity to an equilibrium point R_0 located outside the end of the invariant planes (see Figure 6 (i)). The same holds for $\alpha > 1$ in $O_5 \backslash D$, where $D = \{y = 0\} \cup \{x = z = 0\}$.*
(b) *for $\alpha \in [-2, 1]$, all orbits starting on $O_5 \setminus \{z = 0\}$ go in forward time to infinity to the endpoint R_0 of the positve half-axes of coordinates (z-axes). See Figures 6 (ii) and (iii).*

Theorems 2–5 are proved in section 6. We remark that in order that Figures 4 - 6 are not too crowed, which dificults the comprehension, we have decided to only draw the separatrices of each equilibria. The structure of the paper is as follows. In sections 3 and 4 we describe the dynamics on the Poincaré sphere and on the invariant planes, respectively. In section 5 we provide the results that will be used in the proof of Theorem 1 regarding the α- and ω-limits and finally, we have included an Appendix with both the Poincaré compactification in $\mathbb{R}^2$ and in $\mathbb{R}^3$.

3. Dynamics on the Poincaré sphere $\mathbb{S}^2$

In this section we present the analysis of the flow of system (4) at infinity using the Poincaré compactification of the system in $\mathbb{R}^3$, described in the local charts U_i, V_i for $i = 1, 2, 3$.

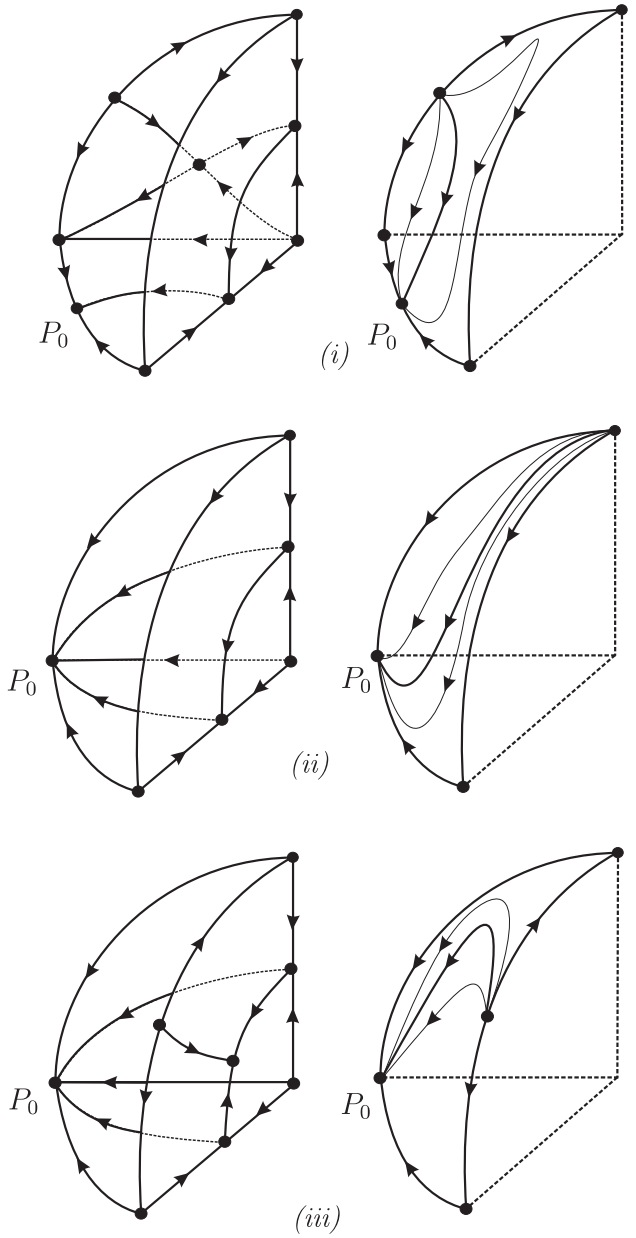

FIGURE 4. Phase portrait of system (4) in the second octant O_2: (i) for $\alpha < -2$ or $\alpha > 1$, (ii) for $\alpha = -2$ or $\alpha = 1$ and (iii) for $-2 < \alpha < 1$. On the left-hand side we draw the phase portrait of system (4) restricted to the invariant planes and on the right-hand side we draw the phase portrait of system (4) on the Poincaré sphere in O_2.

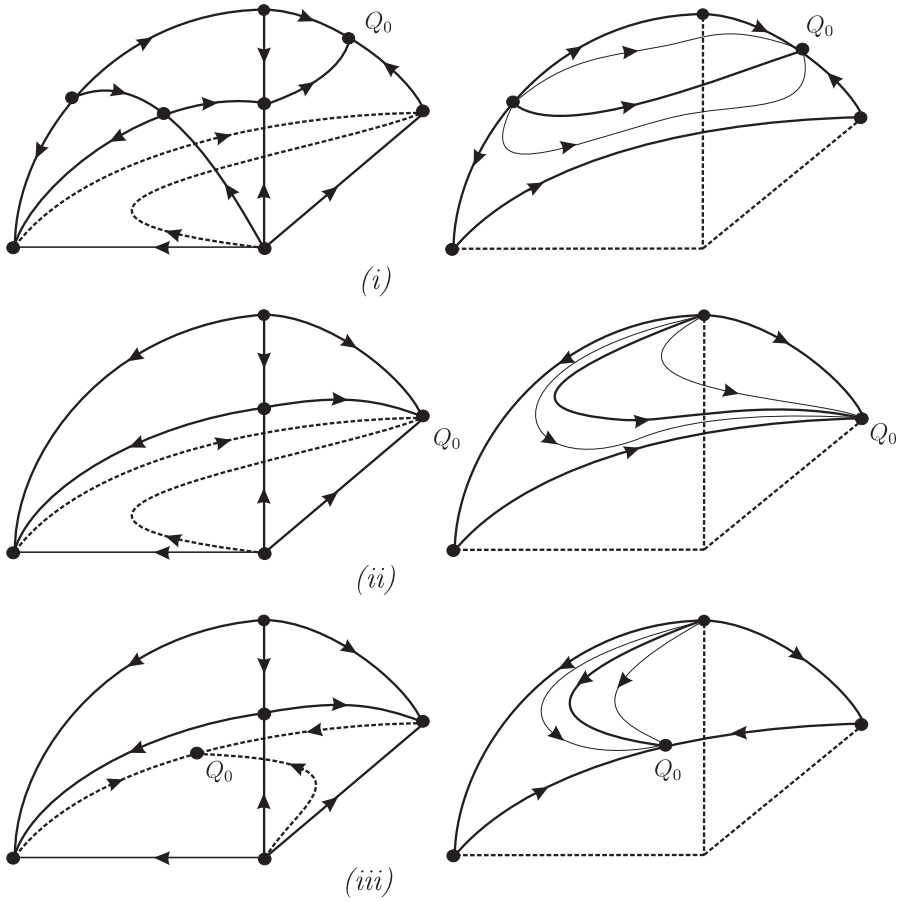

FIGURE 5. Phase portrait of system (4) in the third octant O_3: (i) for $\alpha < -2$ or $\alpha > 1$, (ii) for $\alpha = -2$ or $\alpha = 1$ and (iii) for $-2 < \alpha < 1$. On the left-hand side we draw the phase portrait of system (4) restricted to the invariant planes and on the right-hand side we draw the phase portrait of system (4) on the Poincaré sphere in O_3.

From Appendix 7.2 the expression of the Poincaré compactification $p(X)$ of system (4) in the local chart U_1 is given by

$$\begin{aligned} \dot{z}_1 &= z_1(2 - z_1 - z_2 + \alpha + z_1\alpha - 2z_2\alpha), \\ \dot{z}_2 &= -z_2(-1 - z_1 + 2z_2 + \alpha - 2z_1\alpha + z_2\alpha), \\ \dot{z}_3 &= -z_3(-1 + z_2 + z_3 - z_1\alpha + z_2\alpha). \end{aligned} \tag{5}$$

For $z_3 = 0$ (which correspond to the points on the sphere $\mathbb{S}^2$ at infinity) system (5) becomes

$$\begin{aligned} \dot{z}_1 &= z_1(2 - z_1 - z_2 + \alpha + z_1\alpha - 2z_2\alpha), \\ \dot{z}_2 &= -z_2(-1 - z_1 + 2z_2 + \alpha - 2z_1\alpha + z_2\alpha). \end{aligned} \tag{6}$$

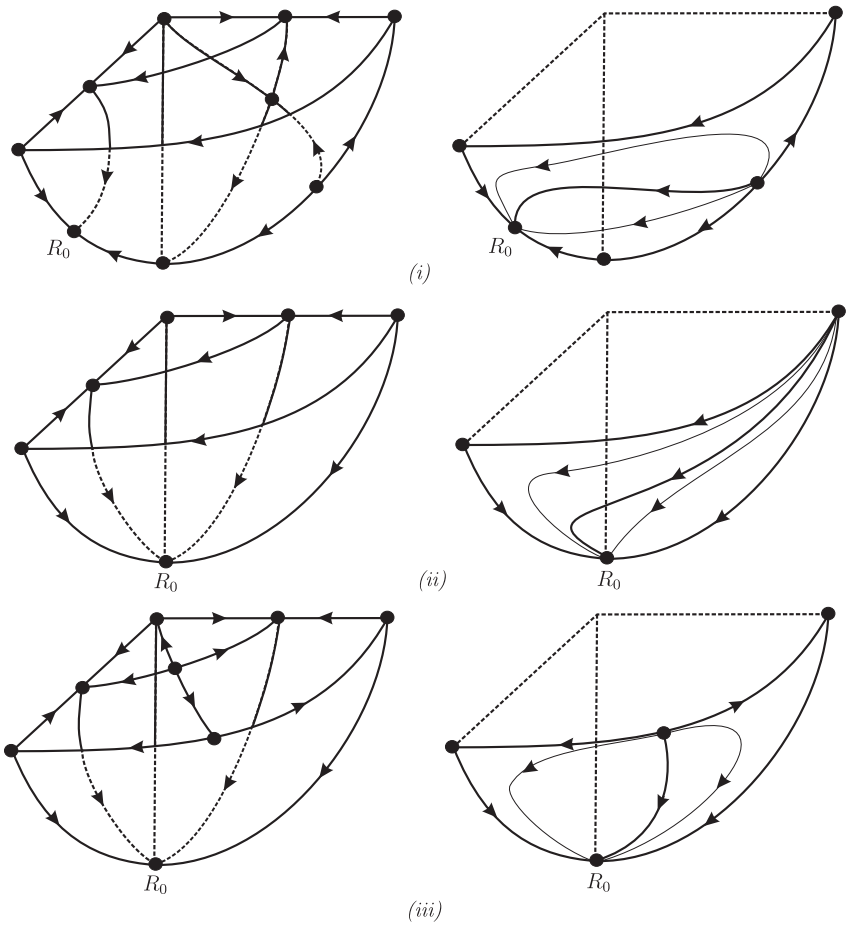

FIGURE 6. Phase portrait of system (4) in the fifth octant O_5: (i) for $\alpha < -2$ or $\alpha > 1$, (ii) for $\alpha = -2$ or $\alpha = 1$ and (iii) for $-2 < \alpha < 1$. On the left-hand side we draw the phase portrait of system (4) restricted to the invariant planes and on the right-hand side we draw the phase portrait of system (4) on the Poincaré sphere in O_5.

System (6) has the following equilibrium points

$$p_1 = (0,0), \quad p_2 = (1,1), \quad p_3 = \left(0\,, \frac{1-\alpha}{2+\alpha}\right), \quad p_4 = \left(\frac{-2-\alpha}{-1+\alpha},\, 0\right).$$

Note that p_3 exists whenever $\alpha \neq -2$ and p_4, whenever $\alpha \neq 1$. The eigenvalues of the Jacobian matrix evaluated in each of the equilibria are $1-\alpha$ and $2+\alpha$ for p_1, $(-3 \pm \sqrt{3i}|(2\alpha-1)|)/2$ for p_2, $-1+\alpha$ and $3(1+\alpha+\alpha^2)/(2+\alpha)$ for p_3, and $-(2+\alpha)$ and $-3(1+\alpha+\alpha^2)/(-1+\alpha)$ for p_4. So, p_2 is a stable focus and, except when $\alpha = 1$ or $\alpha = -2$, these points are hyperbolic, whose topological type depend on the sign of $\alpha - 1$ and $\alpha + 2$.

The flow in the local chart V_1 is the same as the flow in the local chart U_1 because the compacted vector field $p(X)$ in V_1 coincides with the vector field $p(X)$ in U_1 multiplied by -1.

Hence the phase portrait on the chart V_1 is the same as the one in U_1 reserving in an appropriate way the direction of the time.

The expression of the Poincaré compactification $p(X)$ of system (4) in the local chart U_2 is

$$\begin{aligned} \dot{z}_1 &= -z_1(-1+2z_1-z_2+\alpha+z_1\alpha-2z_2\alpha) \\ \dot{z}_2 &= z_2(2-z_1-z_2+\alpha-2z_1\alpha+z_2\alpha), \\ \dot{z}_3 &= -z_3(-1+z_1+z_3+z_1\alpha-z_2\alpha). \end{aligned} \tag{7}$$

System (7) restricted to $z_3 = 0$ becomes

$$\begin{aligned} \dot{z}_1 &= -z_1(-1+2z_1-z_2+\alpha+z_1\alpha-2z_2\alpha) \\ \dot{z}_2 &= z_2(2-z_1-z_2+\alpha-2z_1\alpha+z_2\alpha), \end{aligned} \tag{8}$$

which has the following equilibria

$$q_1 = (0,0), \quad q_2 = (1,1), \quad q_3 = \left(0, -\frac{2+\alpha}{\alpha-1}\right) \text{ and } q_4 = \left(\frac{1-\alpha}{2+\alpha}, 0\right).$$

Note that the equilibria $q_2 = (1,1)$ and $q_4 = (-(-1+\alpha)/(2+\alpha), 0)$ were already studied in the local chart U_1. The eigenvalues of the equilibria q_1 are $1-\alpha$ and $2+\alpha$ and of the equilibria q_3 are $-(2+\alpha)$ and $-3(1+\alpha+\alpha^2)/(2+\alpha)$ for q_3. Again the topological type of these two singular points depend on the sign of $2+\alpha$ and $1-\alpha$ and q_3 does not exist when $\alpha = 1$.

The flow in the local V_2 is the same as the flow in the local chart U_2 reserving in an appropriate way the direction of the time.

The expression of the Poincaré compactification $p(X)$ of system (4) in the local chart U_3 is exactly the same as in in the local chart U_1, due to the symmetry. Consequently, the flow at infinity in the local chart V_3 is the same as the flow in the local chart U_3 and U_1 reversing appropriately the time.

From the study presented in section 3 the topological type of each equilibrium point in the local chart U_i, $i = 1,2,3$ depends on the sign of $\alpha - 1$ and $\alpha + 2$ so we split the study of the dynamics on the Poincaré sphere in five cases: $\alpha < -2$, $\alpha > 1$, $\alpha \in (-2,1)$, $\alpha = -2$ and $\alpha = 1$. In Table 1 we provide the description of the topological type of each equilibria (p_i and q_j, $i = 1,2,3,4$ and $j = 1,3$) according to the value of the parameter α in each the local charts U_1 and U_2, respectively (we recall that the dynamics in U_3 coincide with the one in U_1).

	$\alpha < -2$	$\alpha = -2$	$\alpha \in (-2,1)$	$\alpha = 1$	$\alpha > 1$
p_1	saddle	saddle-node	node	saddle-node	saddle
p_2	unstable focus	unstable focus	unstable focus [1]	unstable focus	unstable focus
p_3	stable node	–	saddle	–	unstable node
p_4	unstable node	–	saddle	–	stable node
q_1	saddle	saddle-node	node	saddle-node	saddle
q_3	unstable node	–	saddle	–	stable node

TABLE 1. Topological type of each equilibria in the local chart U_1 and U_2 according to the value of α, where $p_i \in U_1$, $i = 1,2,3,4$ and $q_j \in U_2$, $j = 1,3$).

From the local behavior of the orbits of system (4) in each local chart of the Poincaré sphere together with the existence of the invariant planes $x = 0$, $y = 0$ and $z = 0$ and because the boundary of the invariant planes at infinity of $\mathbb{R}^3$ are invariant, we get five global phase portraits in the Poincaré sphere, according to the cases studied above. Note that the global phase portraits for $\alpha = -2$ and $\alpha = 1$ are topologically equivalent up to a rescaling of the time, as well as the global phase portraits for $\alpha < -2$ and $\alpha > 1$. In Figure 2 we only draw the non topologically equivalent phase portraits in the Poincaré sphere for system (4).

4. Dynamics of system (4) restricted to the invariant planes

Now we restrict our study to each coordinate plane. On the invariant plane $x = 0$ system (4) becomes

$$\begin{aligned} \dot{y} =& y(1 - y - \alpha z), \\ \dot{z} =& z(1 + (1 + \alpha)y - z). \end{aligned} \tag{9}$$

This system has the following equilibria

$$r_0 = (0, 0), \quad r_1 = (1, 0), \quad r_2 = (0, 1), \quad r_3 = \left(\frac{1 - \alpha}{1 + \alpha + \alpha^2}, \frac{\alpha + 2}{1 + \alpha + \alpha^2} \right).$$

The eigenvalues of the Jacobian matrix evaluated at each of the equilibria are $1, 1$ for r_0; $-1, 2+\alpha$ for r_1; $-1, 1 - \alpha$ for r_2; and $-1, (2 + \alpha)(\alpha - 1)/(1 + \alpha + \alpha^2)$ for r_3. So r_0 is a unstable node and the other points are hyperbolic whose topological type depend on the sign of $\alpha - 1$ and $\alpha + 2$. Note that r_3 coalesces with one of the other equilibria when either $\alpha = -2$ or $\alpha = 1$. The topological type of each of these equilibria is described in Table 2 according to the values of α.

	$\alpha < -2$	$\alpha = -2$	$\alpha \in (-2, 1)$	$\alpha = 1$	$\alpha > 1$
r_0	unstable node	unstable node	unstable node	unstable node	unstable node
r_1	stable node	saddle–node	saddle	saddle	saddle
r_2	saddle	saddle	saddle	saddle–node	stable node
r_3	saddle	–	stable node	–	saddle

Table 2. Topological type of each equilibria in the invariant plane $x = 0$ according to the value of α.

From Appendix 7.1 the expression of the Poincaré compactification of system (9) in the local chart U_1 is

$$\begin{aligned} \dot{z}_1 =& 2z_1 - z_1^2 + z_1\alpha + z_1^2\alpha, \\ \dot{z}_2 =& z_2 - z_2^2 + z_1 z_2 \alpha. \end{aligned}$$

There are two equilibria on $z_2 = 0$, namely $s_0 = (0, 0)$ and $s_1 = ((\alpha + 2)/(1 - \alpha), 0)$. Note that s_1 exists whenever $\alpha \neq 1$ and coalesces with s_0 when $\alpha = -2$. The eigenvalues of the Jacobian matrix evaluated at these two equilibria are $1, (2 + \alpha)$ for s_0 and $-2 - \alpha, (1 + \alpha + \alpha^2)/(1 - \alpha)$ for s_1. Again they are hyperbolic whose topological type depend on the sign of $\alpha - 1$ and $\alpha + 2$.

[1] or node when $\alpha = -1/2$.

The expression of the Poincaré compactification of system (9) in the local chart U_2 is

$$\begin{aligned}\dot{z}_1 =& z_1 - 2z_1^2 - z_1\alpha - z_1^2\alpha,\\ \dot{z}_2 =& z_2 - z_1z_2 - z_2^2 - z_1z_2\alpha.\end{aligned}$$

So the point s_2, the origin of the local chart U_2, is an equilibrium point whose eigenvalues of its Jacobian matrix are $1, 1-\alpha$. The topological types of each of the equilibria in the local charts U_1 and U_2 are described in Table 3 according to the values of α.

	$\alpha<-2$	$\alpha=-2$	$\alpha\in(-2,1)$	$\alpha=1$	$\alpha>1$
s_0	saddle	saddle–node	unstable node	unstable node	unstable node
s_1	unstable node	–	saddle	—	unstable node
s_2	unstable node	unstable node	unstable node	saddle–node	saddle

TABLE 3. Topological type of each equilibria of system (9) in the local chart U_1 and U_2 according to the value of α.

Combining the above analysis in the finite part and at each local chart at infinity for each of the values of α we get five global phase portraits of system (9) in the Poincaré disc. We remark that the global phase portraits when $\alpha>1$ and $\alpha=1$ are topologically equivalent to the cases $\alpha<-2$ and $\alpha=-2$, respectively. So, in Figure 1 we only draw the three non topologically equivalent phase portraits of system (9).

On the invariant plane $y=0$ system (4) becomes

$$\begin{aligned}\dot{x} =& x(1-x+(1+\alpha)z),\\ \dot{z} =& z(1-z-\alpha x).\end{aligned}\tag{10}$$

Such system is equivalent to system (9) by the change of coordinates $(x,z)\to(z,y)$, in other words, the dynamics of system (10) is equivalent to the one of system (9) up to a rotation, see Figure 1.

On the invariant plane $z=0$ system (4) becomes

$$\begin{aligned}\dot{x} =& x(1-x-\alpha y),\\ \dot{y} =& y(1+(1+\alpha)x-y).\end{aligned}\tag{11}$$

Such system is equivalent to system (9) by the change of coordinates $(x,y)\to(y,z)$. So the dynamics of system (11) is topologically equivalent to the dynamics of system (9) up to a rotation and it is drawn in Figure 1.

5. On the ω-limit of the orbits of system (4) on O_1

In this section we provide the ω-limit of all orbits of system (4) in O_1. To do it, we first introduce the notion of ω–limit and α–limit and we state and proof an auxiliary result that will be used to prove the existence of the heteroclinic cycle and of the graph in the positive octant O_1.

Let $\phi_p(t)$ be the solution of system (1) passing through the point $p \in \mathbb{R}^3$, defined on its maximal interval (α_p, ω_p) such that $\phi_p(0) = p$. If $\omega_p = \infty$, we define the *ω-limit set* of p as

$$\omega(p) = \{q \in \mathbb{R}^3 : \exists\{t_n\} \text{ with } t_n = \infty \text{ and } \phi_p(t_n) = q \text{ when } n = \infty\}.$$

In the same way, if $\alpha_p = -\infty$, we define the *α-limit set* of p as

$$\alpha(p) = \{q \in \mathbb{R}^3 : \exists\{t_n\} \text{ with } t_n = -\infty \text{ and } \phi_p(t_n) = q \text{ when } n = \infty\}.$$

For more details on the ω– and α–limit sets see for instance section 1.4 of [4].

The existence of a Darboux invariant of system (1) provides information about the ω– and α–limit sets of all orbits of system (1). More precisely, we have the following result, where the definition of Poincaré compactification and Poincaré sphere is given in subsection 7.2. Its proof can be found in [9] for the 2-dimensional case so here we repeat it for the 3-dimensional case.

Proposition 6. *Let $\mathbb{S}^2$ be the infinity of the Poincaré sphere and $I(x, y, z, t) = f(x, y, z)e^{st}$ be a Darboux invariant of system (1). Let also $p \in \mathbb{R}^3$ and $\phi_p(t)$ be the solution of system (1) with maximal interval (α_p, ω_p) such that $\phi_p(0) = p$. If $\omega_p = \infty$ then $\omega(p) \subset \{f(x, y, z) = 0\} \cup \mathbb{S}^2$ and if $\alpha_p = -\infty$ then $\alpha(p) \subset \{f(x, y, z) = 0\} \cup \mathbb{S}^2$.*

Proof. Here we prove the first statement in the proposition since the second one follows in the same lines. Assume that $s > 0$ and let $\phi_p(t) = (x_p(t), y_p(t), z_p(t))$. Since $I(x, y, z, t)$ is an invariant $I(x_p(t), y_p(t), z(t)t) = a \in \mathbb{R}$ for all $t \in (\alpha_p, \omega_p)$. Then

$$a = \lim_{t\to\infty} I(x_p(t), y_p(t), z_p(t), t) = \lim_{t\to\infty} f(x_p(t), y_p(t), z_p(t))e^{st}.$$

As $\lim_{t\to\infty} e^{st} = \infty$, we have that $\lim_{t\to\infty} f(x_p(t), y_p(t), z_r(t)) = 0$. So, by continuity and the definition of ω–limit set it follows that $\omega(\mathrm{p}) \subset \{f(x, y, z) = 0\}$, and for the α–limit set $\alpha(p) \in \mathbb{S}^2$. □

Now we shall provide the ω-limit of all orbits of system (4) in O. For this, we will distinguish between the cases $\alpha \leq -2$ and $\alpha \in (-2, 1)$. The results for $\alpha \geq 1$ are the same as the ones for $\alpha \leq -2$ since the dynamics is the same reversing the time.

Proposition 7. *Assume $\alpha \leq 2$. There exists a separatrix cycle F formed by orbits connecting the finite equilibrium points on the boundary of O_1 and every orbit on O_1 has F as the ω-limit.*

Proof. Let $V(x, y, z) = x + y + z$ and denote by $\gamma(t) = (x(t), y(t), z(t))$ an orbit of system (4). We define $V(t) = V(\gamma(t))$ and

$$\dot{V} = \frac{dV}{dt}(\gamma(t)) = \frac{\partial V}{\partial x}x(1-x-\alpha y+(1+\alpha)z)+\frac{\partial V}{\partial y}y(1+(1+\alpha)x-y-\alpha z)+\frac{\partial V}{\partial z}z(1-\alpha x+(1+\alpha)y-z).$$

Hence

$$\dot{V} = x + y + z - (x^2 + y^2 + z^2 + xy + xz + yz).$$

Applying the change of coordinates

$$x \to \frac{1}{3}(3w - 1), \quad y \to \frac{1}{3}(3w - 3v - 3u + 2), \quad z \to \frac{1}{3}(3w - 6u + 2)),$$

the set $\{(x,y,z)\in\mathbb{R}^3 : \dot{V}=0\}$ is the elliptic paraboloid

$$E=\{(u,v,w)\in\mathbb{R}^3 : 3w-3u^2-v^2=0\}.$$

Clearly $\dot{V}=0$ on the paraboloid E that contains the equilibrium points $(1,0,0),(0,1,0)$ and $(0,0,1)$. On that equilibria the function V is equal to 1. Moreover,

$$\begin{aligned}\dot{V} &= x+y+z-(x^2+y^2+z^2+xy+xz+yz)\\ &\leq x+y+z-(x^2+y^2+z^2+2xy+2xz+2yz)\\ &= V-V^2=V(1-V).\end{aligned}$$

So, $\dot{V}<0$ on $V>1$. Taking this into account, that the points of the interior of O_1 satisfying $\dot{V}=0$ are the ones on E and that V on the above equilibrium points is equal to one, we conclude that every orbit in the interior of O_1 enters, and remains inside, the set

$$S=\{(x,y,z)\in O_1^+ : 0<V\leq 1\}.$$

Furthermore, in view of Theorem 1 *(c)* all orbits in S approach Ω, so all orbits on O_1 approach $S\cap\Omega$ and have their $\omega-$limit in this set. In view of the Poincaré-Bendixson theorem and that the equilibria $(1,0,0),(0,1,0)$ and $(0,0,1)$ can not be the $\omega-$ limit of any orbit because they are saddles, the unique possibility is to be the heteroclinic cycle F formed by orbits connecting the equilibrium points $(1,0,0),(0,1,0)$ and $(0,0,1)$. This proves the existence of the separatrix cycle F as stated in the proposition. □

Proposition 8. *Assume $\alpha\in(-2,1)$. There exists a graph G formed by orbits connecting the finite equilibrium points on O_1, except the origin. The $\omega-$limit set of all orbits on O_1 is the set formed by the three equilibria that are not on the half-positive axes.*

Proof. Consider V as in the proof Proposition 7. Proceeding in the same manner as in that proof, we have that the points of the interior of O_1 satisfying $\dot{V}=0$ are the ones on the paraboloid E, that V on the equilibrium points $(1,0,0),(0,1,0),(0,0,1)$ is equal to 1 and that V on the equilibrium points

$$P_1=\frac{1}{1+\alpha+\alpha^2}(0,\alpha-1,\alpha+2),\ P_2=\frac{1}{1+\alpha+\alpha^2}(\alpha-1,\alpha+2,0),\ P_3=\frac{1}{1+\alpha+\alpha^2}(\alpha+2,0,\alpha-1)$$

is equal to $3/(1+\alpha+\alpha^2)>1$. So, as in the proof of Proposition 7, every orbit in the interior of O_1 enters, and remains inside, the set

$$S_1=\{(x,y,z)\in O_1^+ : 0<V\leq 3/(1+\alpha+\alpha^2)\}.$$

Furthermore, in view of Theorem 1 *(c)* all orbits in S_1 approach Ω, so all orbits on O_1^+ approach $S_1\cap\Omega$ and have their $\omega-$limit in this set. In view of the Poincaré-Bendixson theorem and that the equilibria $(1,0,0),(0,1,0)$ and $(0,0,1)$ can not be the $\omega-$ limit of any orbits because they are saddles, the unique possibility is to be either P_1, or P_2, or P_3. This guarantees the existence of the graph G as in the statement of the proposition. □

6. Proofs of Theorems 1–5

Proof of Theorem 1. Taking into account that $\alpha+\beta \neq 2$ and $\alpha \neq \beta$ it follows easily from (3) that the unique irreducible invariant planes of system (1) are $f_1(x,y,z) = x = 0$, $f_2(x,y,z) = y = 0$ and $f_3(x,y,z) = z = 0$. Moreover, the $f_1(x,y,z) = 0$, $f_2(x,y,z) = 0$ and $f_3(x,y,z) = 0$ have cofactors, $1-x-\alpha y-\beta z$, $1-\beta x-y-\alpha z$ and $1-\alpha x-\beta y-z$, respectively. Hence, system (1) admits a Darboux invariant of the form $I(x,y,z,t) = e^{st}f(x,y,z)$, with $f = f_1^{r_1}f_2^{r_2}f_3^{r_3}$, if and only if, equation (2) is satisfied for a real $s \neq 0$. Doing so we get

$$s = -3r_2, \quad r_1 = r_3 = r_2 \quad \text{and} \quad \alpha+\beta+1 = 0.$$

Choosing $r_2 = 1$ we have $s = -3$ and $r_1 = r_2 = r_3 = 1$, being the Darboux invariant $I = e^{-3t}xyz$. This concludes the proof of Theorem 1*(a)*.

Statement *(b)* can be easily checked and statement *(c)* follows from Proposition 6 and the expression of the Darboux invariant obtained in statement *(a)*. □

Proof of Theorem 2. The proof of statement *(a)* of Theorem 2 follows directly from the study done in section 3.

To prove statement *(b)* we note that since the planes of coordinates and the sphere at infinity are invariant, the intersection if formed by orbits.

If $\alpha \leq -2$ the open arc of the infinity of O_1 in the local chart U_1 corresponding to the end of the plane $z = 0$ is formed by an orbit having as α-limit the equilibrium $(0,0,0)$. The open arc of the infinity of O_1 corresponding to the end of the plane $y = 0$ is formed by an orbit having as ω-limit the equilibrium $(0,0,0)$. The orbit on the x-axes near of $(0,0,0)$ has this equilibrium as its ω-limit. Similar studies can be done for the equilibria located at the origin of the local charts U_2 and U_3 that is, at the end of the y- and z-axes, respectively. Hence the boundary of the infinity of O_1 is formed by a heteroclinic cycle formed by three equilibria coming from the ones located at the end of the positive half-axes, and the three orbits living on the three open arcs connecting these three points and contained in the boundary of the infinity of O_1. From the study of the global dynamics on the Poincaré sphere in section 3 we see that there is an additional equilibria in the interior of the heteroclinic cycle that is an stable attractor and it is the ω-limit set of each point on the interior of the heteroclinic cycle. This completes the proof of statement *(b.1)*. The orientation of the heteroclinic cycle is reversed for the case $\alpha \geq 1$.

If $-2 < \alpha < 1$, as shown in section 3 there are three additional equilibria on the open arcs connecting the end of the invariant planes. In the local chart U_1 the middle equilibria in the x-axis is the ω-limit of the equilibrium at the end of the plane $z = 0$ and of $(0,0,0)$. The same happens on the y-axis. Similar studies can be done for the y-axis on the local charts U_2 and for the equilibrium at the end of the z-axis in the local chart U_3. Thus the boundary of the infinity of O_1 is formed by a graph formed by six equilibria coming from the ones located at the positive half-axes, and the six orbits living on the six open arcs connecting these six points and contained in the boundary of the infinity of O_1. From the study of the global dynamics on the Poincaré sphere made in section 3 we see that there is an additional equilibrium point in the interior of the graph. It is an stable attractor and it is the ω-limit set of each point on the interior of the graph. This completes the proof of statement *(b.2)*.

The proof concerning the $\omega-$limit part of statement *(c.1)* follows directly from Proposition 7. Combining the results from sections 3 and 9 we get the phase portraits in Figure 3. From them and the existence of the separatrix cycle F we conclude the proof of statement *(c.1)*.

The proof concerning the $\omega-$limit part of statement *(c.2)* follows directly from Proposition 8. Combining the results from sections 3 and 9 we get the phase portraits in Figure 4. From them and the existence of the graph G we conclude the proof of statement *(c.2)*. Hence, the proof of Theorem 2 is concluded. □

Proof of Theorems 3–5. Combining the analysis of the dynamics in the Poincaré sphere and in each invariant plane obtained in sections 3 and 9, respectively, we get the global phase portraits of system (4) in each octant given in Figures 4-6. We note that these are all possible phase portraits up to a rotation (see Theorem 1 *(b)*). The behavior in forward time of all orbits in each octant described in Theorems 3 to 5 follow directly from the previous analysis and the Poincaré Bendixson theorem (see again Figures 4-6). The proof of Theorems 3 to 5 is complete. □

7. Appendix

7.1. **Poincaré compactification in $\mathbb{R}^2$.** Let $X = (P_1(x, y), P_2(x, y))$ be a planar polynomial vector field of degree $n = max\{deg(P_i) : i = 1, 2\}$. The *Poincaré compactified vector field* $p(X)$ corresponding to X is an analytic vector field induced on $\mathbb{S}^2$ as follows (for more details, see [4]).

Let $\mathbb{S}^2 = \{y = (y_1, y_2, y_3) \in \mathbb{R}^3;\ y_1^2 + y_2^2 + y_3^2 = 1\}$ and $T_y\mathbb{S}^2$ be the tangent plane to $\mathbb{S}^2$ at point y. We identify $\mathbb{R}^2$ with $T_{(0,0,1)}\mathbb{S}^2$ and we consider the central projection $f : T_{(0,0,1)}\mathbb{S}^2 = \mathbb{S}^2$. The map f defines two copies of X on $\mathbb{S}^2$, one in the southern hemisphere and the other in the northern hemisphere. Denote by $\bar{X}$ the vector field $D(f \circ X)$ defined on $\mathbb{S}^2 \setminus \mathbb{S}^1$, where $\mathbb{S}^1 = \{y \in \mathbb{S}^2;\ y_3 = 0\}$ is identified with the infinity of $\mathbb{R}^2$.

For extending $\bar{X}$ to a vector field on $\mathbb{S}^2$, including $\mathbb{S}^1$, X must satisfy convenient conditions. Since the degree of X is n, $p(X)$ is the unique analytic extension of $y_3^{n-1}\bar{X}$ to $\mathbb{S}^2$. On $\mathbb{S}^2 \setminus \mathbb{S}^1$ there is two symmetric copies of X, and once we know the behavior of $p(X)$ near $\mathbb{S}^1$, we know the behavior of X in a neighborhood of the infinity. The Poincaré compactification has the property that $\mathbb{S}^1$ is invariant under the flow of $p(X)$. The projection of the closed northern hemisphere of $\mathbb{S}^2$ on $y_3 = 0$ under $(y_1, y_2, y_3) \mapsto (y_1, y_2)$ is called the *Poincaré disc*, and its boundary is $\mathbb{S}^1$.

Two polynomial vector fields X and Y on $\mathbb{R}^2$ are *topologically equivalent* if there exists a homeomorphism on $\mathbb{S}^2$, preserving the infinity $\mathbb{S}^1$, carrying orbits of the flow induced by $p(X)$ into orbits of the flow induced by $p(Y)$ preserving or not the orientation of all orbits.

As $\mathbb{S}^2$ is a differentiable manifold, in order to compute the explicit expression of $p(X)$, we consider six local charts $U_i = \{y \in \mathbb{S}^2;\ y_i > 0\}$ and $V_i = \{y \in \mathbb{S}^2;\ y_i < 0\}$, where $i = 1, 2, 3$, and the diffeomorphisms $F_i : U_i = \mathbb{R}^2$ and $G_i : V_i = \mathbb{R}^2$, for $i = 1, 2, 3$, which are the inverses of the central projections from the tangent planes at the points $(1, 0, 0)$, $(-1, 0, 0)$, $(0, 1, 0)$, $(0, -1, 0)$, $(0, 0, 1)$ and $(0, 0, -1)$, respectively. After some computations and a rescaling of the time, $p(X)$

in the local charts U_1 and U_2 is given, respectively, by:

$$z_2^n\left(P_2 - z_1P_1, -z_2P_1\right), \quad \text{where } P_i = P_i(1/z_2, z_1/z_2),$$
$$z_2^n\left(P_1 - z_2P_2, -z_1P_2\right), \quad \text{where } P_i = P_i(z_1/z_2, 1/z_2).$$

The expression for $p(X)$ in U_3 is $z_2^n(P_1, P_2)$ and the expression for $p(X)$ in V_i's are the same as that for U_i's but multiplied by the factor $(-1)^{n-1}$. In these coordinates $z_2 = 0$ always denotes the points of the infinity $\mathbb{S}^1$.

7.2. **Poincaré compactification in $\mathbb{R}^3$.** Let $X = (P_1(x, y, z), P_2(x, y, z), P_3(x, y, z))$ be a planar polynomial vector field of degree $n = max\{deg(P_i) : i = 1, 2, 3\}$ and let

$$\mathbb{S}^3 = \{y = (y_1, y_2, y_3, y_4) : ||y|| = 1\},\ \mathbb{S}_+ = \{y \in \mathbb{S}^3 : y_4 > 0\},\ \mathbb{S}_- = \{y \in \mathbb{S}^3 : y_4 < 0\}$$

be, respectively, the unit sphere in $\mathbb{R}^4$, the northern hemisphere of $\mathbb{S}^3$ and the southern hemisphere of $\mathbb{S}^3$. The tangent space of $\mathbb{S}^3$ at the point y will be denoted by $T_y\mathbb{S}^3$ and the tangent plane $T_{(0,0,0,1)}\mathbb{S}^3 = \{(x_1, x_2, x_3, 1) \in \mathbb{R}^4 : (x_1, x_2, x_3) \in \mathbb{R}^3\}$ can be identified with $\mathbb{R}^3$.

Consider the central projections

$$f_\pm\colon \mathbb{R}^3 = T_{(0,0,0,1)}\mathbb{S}^3 \to \mathbb{S}_\pm, \quad f_\pm(x) = \pm\frac{(x_1, x_2, x_3, 1)}{\Delta(x)} \quad \text{with} \quad \Delta(x) = \left(1 + \sum_{i=1}^{3} x_i^2\right)^{1/2}.$$

Using these central projections, $\mathbb{R}^3$ is identified with $\mathbb{S}_+$ and $\mathbb{S}_-$. Note that the equator of $\mathbb{S}^3$ is $\mathbb{S}^2 = \{y \in \mathbb{S}^3 : y_4 = 0\}$.

The maps $f_\pm$ define two copies of X on $\mathbb{S}^3$, one $Df_+ \circ X$ in $\mathbb{S}_+$, and the other, $Df_- \circ X$ in $\mathbb{S}_-$. Denote by $\overline{X}$ the vector field on $\mathbb{S}^3 \setminus \mathbb{S}^2 = \mathbb{S}_+ \cup \mathbb{S}_-$, that restricted to $\mathbb{S}_+$ coincides with $Df_+ \circ X$, and restricted to $\mathbb{S}_-$ coincides with $Df_- \circ X$. We can extend analytically the vector field $\overline{X}(y)$ to the whole sphere $\mathbb{S}^3$ setting $p(X) = y_4^{n-1}\overline{X}(y)$. This extended vector field $p(X)$ is called the Poincaré compactification of X on $\mathbb{S}^3$.

Using that $\mathbb{S}^3$ is a differentiable manifold, to compute the expression for $p(X)$, we can consider the eight local charts (U_i, F_i), (V_i, G_i), where

$$U_i = \{y \in \mathbb{S}^3 : y_i > 0\} \quad \text{and} \quad V_i = \{y \in \mathbb{S}^3 : y_i < 0\}, \quad \text{for } i = 1, 2, 3, 4.$$

Note that the diffeomorphisms $F_i\colon U_i \to \mathbb{R}^3$ and $G_i\colon V_i \to \mathbb{R}^3$ for $i = 1, 2, 3, 4$ are the inverse of the central projections from the origin to the tangent hyperplane at the points $(\pm1, 0, 0, 0)$, $(0, \pm1, 0, 0)$, $(0, 0, \pm1, 0)$ and $(0, 0, 0, \pm1)$, respectively.

Assume that $(0, 0, 0, 0)$, $(y_1, y_2, y_3, y_4) \in \mathbb{S}^3$ and $(1, z_1, z_2, z_3)$ in the tangent hyperplane to $\mathbb{S}^3$ at $(1, 0, 0, 0)$ are collinear. Then we have $1/y_1 = z_1/y_2 = z_2/y_3 = z_3/y_4$ and, so $F_1(y) = (y_2/y_1, y_3/y_1, y_4/y_1) = (z_1, z_2, z_3)$ defines the coordinates on U_1. As

$$DF_1(y) = \begin{pmatrix} -y_2/y_1^2 & 1/y_1 & 0 & 0 \\ -y_3/y_1^2 & 0 & 1/y_1 & 0 \\ -y_4/y_1^2 & 0 & 1/y_1 & 0 \end{pmatrix}$$

and $y_4^{n-1} = (z_3/\Delta(z)^{n-1})$, the analytical vector field $p(X)$ in the local chart U_1 becomes, after a rescaling of the time variable,

$$z_3^n\big(-z_1P_1+P_2,-z_2P_1+P_3,z_3P_1\big), \quad \text{where } P_i = P_i(1/z_3, z_1/z_3, z_2/z_3).$$

Similarly, the expressions of $p(X)$ in U_2 and U_3, after a rescaling of the time variable, are, respectively,

$$z_3^n\big(-z_1P_2+P_1,-z_2P_2+P_3,z_3P_2\big), \quad \text{where } P_i = P_i(z_1/z_3, 1/z_3, z_2/z_3),$$
$$z_3^n\big(-z_1P_3+P_1,-z_2P_3+P_2,z_3P_3\big), \quad \text{where } P_i = P_i(z_1/z_3, z_2/z_3, 1/z_3).$$

The expression for $p(X)$ in U_4 is $z_3^{n+1}(P_1,P_2,P_3)$ and the expression for $p(X)$ in V_i is the same as in U_i multiplied by $(-1)^{n-1}$, for all $i = 1,2,3,4$.

From now on we will consider only the orthogonal projection of $p(X)$ from $\mathbb{S}_+$ to $y_4 = 0$ and we will denote it again by $p(X)$. Observe that the projection of the closed $\mathbb{S}_+$ is a closed ball of radius one, denoted by B, whose interior is diffeomorphic to $\mathbb{R}^3$. Its boundary, $\mathbb{S}^2$, corresponds to the infinity of $\mathbb{R}^3$. Moreover, $p(X)$ is defined in the whole closed ball B in such way that the flow on the boundary, given by $z_3 = 0$ is invariant. The vector field induced by $p(X)$ on B is called the Poincaré compactification of X and B is called the Poincaré sphere.

We recall that two polynomial vector fields X and Y on $\mathbb{R}^3$ are *topologically equivalent* if there exists a homeomorphism on $\mathbb{S}^3$, preserving the infinity $\mathbb{S}^2$, carrying orbits of the flow induced by $p(X)$ into orbits of the flow induced by $p(Y)$ preserving or not the orientation of the orbits.

Acknowledgements

The first author is partially supported by FAPESP grants "Projeto Temático" 2014/00304-2 and project number 2017/20854-5. The second author is partially supported by FCT/Portugal through UID/MAT/ 04459/2013.

References

[1] A. Battauz and F. Zanolin *Coexistence states for periodic competitive Kolmogorov system*, J. Math. Anal. Appl. **219** (1998), 179–199.
[2] G. Blé, V. Castellanos, J. Llibre and I. Quilantán *Integrability and global dynamics of the May-Leonard model*, Nonlinear Anal. Real World Appl. **14** (2013), 280–293.
[3] F.H. Busse *Transition to turbulence via the statistical limit cycle rout*, Syneretics, Springer-Verlag, Berlin, 1978.
[4] F. Dumortier, J. Llibre and J. C. Artés *Qualitative Theory of Planar Differential Systems*, UniversiText, Springer-verlag, New York, 2006.
[5] P. Glansdorff and I. Prigogine *Thermodynamic theory of structure, stability and fluctuations*, John Wiley & Sons Ltd, London 1971.
[6] R. Hannesson *Optimal harvesting of ecologically interdependent fish species*, J. Environ. Econ. Manag. **10** (1983), 329–345.
[7] A. Kolmogorov *Sulla teoria di Volterra della lotta per l'esistenza*, G. Ist. Ital. Degli Attuari **7** (1936), 74–80.
[8] G. Laval and R. Pellat *Plasma Physics*. Proceedings of Summer School of Theoretical Physics, Gordon and Breach, New York, 1975.
[9] J. Llibre and R. Oliveira *Quadratic systems with invariant straight lines of total multiplicity two having Darboux invariants*. Commun. Contemp. Math. **17** (2015), 1450018, 17 pp.

[10] J. Llibre and X. Zhang *Dynamics of some three-dimensional Lotka-Volterra systems*, Mediterranean J. Math. **14** (2017), 126–139.
[11] A.J. Lotka *Analytical note on certain rhythmic relations in organic systems*, Proc. Natl. Acad. Sci. USA **6** (1920), 410–415.
[12] R. M. May *Stability and Complexity in Model Ecosystems*, Princeton, New Jersey, 1974.
[13] R.M. May and W.J. Leonard *Nonlinear aspects of competition between three species*, SIAM J. Appl. Math. **29** (1975), 243–253.
[14] P. Schuster, K. Sigmund and R. Wolf *On ω-limits for competition between three species*, SIAM J. Math. **37** (1979), 49–54.
[15] V. Volterra *Lecons sur la Théorie Mathématique de la Lutte pour la vie*, Gauthier-Villars, Paris, 1931.

[1] Departamento de Matemática, ICMC-Universidade de São Paulo, Avenida Trabalhador São-carlense, 400 - 13566-590, São Carlos, SP, Brazil

E-mail address: regilene@icmc.usp.br

[2] Departamento de Matemática, Instituto Superior Técnico, Universidade Técnica de Lisboa, Av. Rovisco Pais 1049–001, Lisboa, Portugal

E-mail address: cvalls@math.ist.utl.pt